© 2022. Published by The Company of Biologists Ltd | Development (2022) 149, dev200275. doi:10.1242/dev.200275

STEM CELLS AND REGENERATION

RESEARCH ARTICLE

Notch signaling regulates neural stem cell quiescence entry and exit in *Drosophila*

Chhavi Sood, Virginia T. Justis, Susan E. Doyle and Sarah E. Siegrist*

ABSTRACT

Stem cells enter and exit quiescence as part of normal developmental programs and to maintain tissue homeostasis in adulthood. Although it is clear that stem cell intrinsic and extrinsic cues, local and systemic, regulate quiescence, it remains unclear whether intrinsic and extrinsic cues coordinate to control quiescence and how cue coordination is achieved. Here, we report that Notch signaling coordinates neuroblast intrinsic temporal programs with extrinsic nutrient cues to regulate quiescence in *Drosophila*. When Notch activity is reduced, quiescence is delayed or altogether bypassed, with some neuroblasts dividing continuously during the embryonic-to-larval transition. During embryogenesis before quiescence, neuroblasts express Notch and the Notch ligand Delta. After division, Delta is partitioned to adjacent GMC daughters where it transactivates Notch in neuroblasts. Over time, in response to intrinsic temporal cues and increasing numbers of Delta-expressing daughters, neuroblast Notch activity increases, leading to cell cycle exit and consequently, attenuation of Notch pathway activity. Quiescent neuroblasts have low to no active Notch, which is required for exit from quiescence in response to nutrient cues. Thus, Notch signaling coordinates proliferation versus quiescence decisions.

KEY WORDS: Notch signaling, Neural stem cell, Quiescence, Neuroblast, Delta, Tribbles, Hippo, PI3-kinase, Dacapo, Asymmetric cell division, Cell cycle, *Drosophila*

INTRODUCTION

Most stem cells in adult tissues remain in a poised, non-proliferative state known as quiescence. Quiescence, typically thought of as G0 arrest, is associated with reduced transcription, translation and ribosome biogenesis and, more recently, with increased lysosomal activity and fatty acid utilization (Kalucka et al., 2018; Coller, 2019; Kobayashi et al., 2019). In adults, stem cells reactivate from quiescence to maintain tissue homeostasis and for repair, whereas in development, quiescence is 'pre-programmed' and required to ensure that sufficient dietary nutrients or other key factors are available to fuel cell divisions needed to support continued growth (Cheung and Rando, 2013; Cavallucci et al., 2016; Kalamakis et al., 2019; Cho et al., 2019; Urbán et al., 2019). Although stem cell entry and exit from quiescence is important in development and adulthood, mechanisms and the cell signaling pathways that regulate quiescence entry and exit are incompletely understood (Li et al., 2017; Mohammad et al., 2019; Sueda and Kageyama, 2020).

In *Drosophila*, neural stem cells, known as neuroblasts (NBs), enter and exit quiescence at defined developmental times (Ito and Hotta, 1992; Truman and Bate, 1988; Britton and Edgar, 1998; Tsuji et al., 2008; Chell and Brand, 2010; Sousa-Nunes et al., 2011; Sipe and Siegrist, 2017; Yuan et al., 2020). In the central brain (CB), all NBs, except for a small subset, enter quiescence at the end of embryogenesis, coincident with declining maternal nutrient stores, and then reactivate after newborn larvae consume their first complete meal (Britton and Edgar, 1998; Chell and Brand, 2010; Sousa-Nunes et al., 2011; Sipe and Siegrist, 2017; Yuan et al., 2020). In response to animal feeding, PI3-kinase becomes active in NBs, their cortex glial niche and trachea, leading to coordinated increases in cell growth, endoreplication of glia and trachea, and resumption of NB divisions (Chell and Brand, 2010; Sousa-Nunes et al., 2011; Sipe and Siegrist, 2017; Spéder and Brand, 2018; Yuan et al., 2020). Concurrent with nutrient-dependent PI3-kinase activation, Yorkie, a transcriptional co-activator negatively regulated by Hippo signaling, localizes to the NB nucleus to promote growth (Ding et al., 2016). When PI3-kinase activity is reduced NB reactivation is delayed and, when Hippo activity is reduced, NBs reactivate prematurely (Chell and Brand, 2010; Sousa-Nunes et al., 2011; Ding et al., 2016; Yuan et al., 2020). Although dietary nutrients and growth signaling are key extrinsic cues required for NB reactivation, it remains unclear how extrinsic cues coordinate with NB intrinsic cues to control quiescence.

A low-level pulse of the homeodomain transcription factor Prospero (Pros) triggers quiescence, and timing of the Pros pulse is regulated by NB intrinsic temporal factors (Lai and Doe, 2014). Pros is usually partitioned asymmetrically to ganglion mother cells (GMC) after NBs divide, where it functions to promote GMC cell cycle exit (Hirata et al., 1995; Choksi et al., 2006; Colonques et al., 2011). In *nubbin/pdm2* mutants, the NB Pros pulse and quiescence occur prematurely, whereas in *castor* (*cas*) mutants, the NB Pros pulse and quiescence are delayed (Tsuji et al., 2008; Lai and Doe, 2014). Nubbin/Pdm2 and Cas are both temporal factors and are expressed sequentially in embryonic NBs. Dacapo (dap), a cyclin-dependent kinase inhibitor, and tribbles (trbl), a protein kinase that inhibits both insulin signaling activity and String (stg), also are reported to regulate NB quiescence (Colonques et al., 2011; Otsuki and Brand, 2018, 2019). But how cell cycle gene regulation is coupled with temporal factor expression and Pros is not yet understood. Nor is it clear whether other factors are required.

From a large-scale RNAi screen aimed at identifying genes that regulate neural stem cell proliferation decisions during development, we identified Notch, an evolutionarily conserved transmembrane receptor that functions in cell-cell communication. In *Drosophila*, there is one Notch receptor and two Notch ligands, Delta and Serrate (Rebay et al., 1991; Fiuza and Arias, 2007; Kopan and Ilagan, 2009). Notch is activated after the Notch receptor binds

Department of Biology, University of Virginia, Charlottesville, VA 22904, USA.

*Author for correspondence (ses4gr@virginia.edu)

C.S., 0000-0002-3813-5774; S.E.S., 0000-0003-0685-5387

Handling Editor: Thomas Lecuit
Received 17 October 2021; Accepted 13 January 2022

Development (2022) 149, dev200275. doi:10.1242/dev.200275

its ligand expressed on neighboring cells. After ligand binding, Notch is proteolytically cleaved, first by Kuzbanian (Kuz), an ADAM metalloprotease, and then by γ-secretase, resulting in a liberated, cleaved and active form of Notch, known as Notch ICD (Notch intracellular domain). Notch ICD translocates to the nucleus to regulate gene expression through interactions with Suppressor of Hairless [Su(H)] and the transcriptional co-activator Mastermind (Fortini and Artavanis-Tsakonas, 1994; Pan and Rubin, 1997; De Strooper et al., 1999; Mumm et al., 2000; Kopan and Ilagan, 2009). Context-dependent Notch signaling can determine cellular proliferation status by regulating expression of cell cycle inhibitors such as Dap and cell cycle activators such as Cyclin E, String and E2f (Sriuranpong et al., 2001; Deng et al., 2001; Noseda et al., 2004; Herranz et al., 2008; Ishikawa et al., 2008; Bivik et al., 2016). Here, we show that Notch pathway activity increases in NBs during embryogenesis and that high Notch triggers quiescence entry. As a consequence of quiescence and cell cycle exit, Notch signaling becomes attenuated and low Notch is required for NBs to exit quiescence in response to dietary nutrient cues.

RESULTS

Notch signaling positively regulates CB NB quiescence

All neuroblasts in the central brain, except for a small subset, stop proliferating at two defined times in development. First, during the embryonic-to-larval transition when most CB NBs enter quiescence (Fig. 1A) (Tsuji et al., 2008; Lai and Doe, 2014; Otsuki and Brand, 2018). Second, within 24 h after pupal formation, when most CB NBs either terminally differentiate or undergo cell death (Ito and Hotta, 1992; Truman and Bate, 1988; Maurange et al., 2008; Siegrist et al., 2010; Homem et al., 2014; Yang et al., 2017). From a large-scale RNAi screen aimed at identifying genes regulating termination of neurogenesis in the CB during pupal stages, we identified Notch and Notch pathway components (Pahl et al., 2019). To better understand how neurogenesis terminates, we asked whether Notch signaling is also required for CB NB quiescence during the embryonic-to-larval transition.

At 0 h after larval hatching (ALH), the majority of CB NBs are small and quiescent, except for a subset, which include the four mushroom body (MB) NBs located on the dorsal surface (designated 1-4 in all confocal images) and the ventro-lateral (VL)

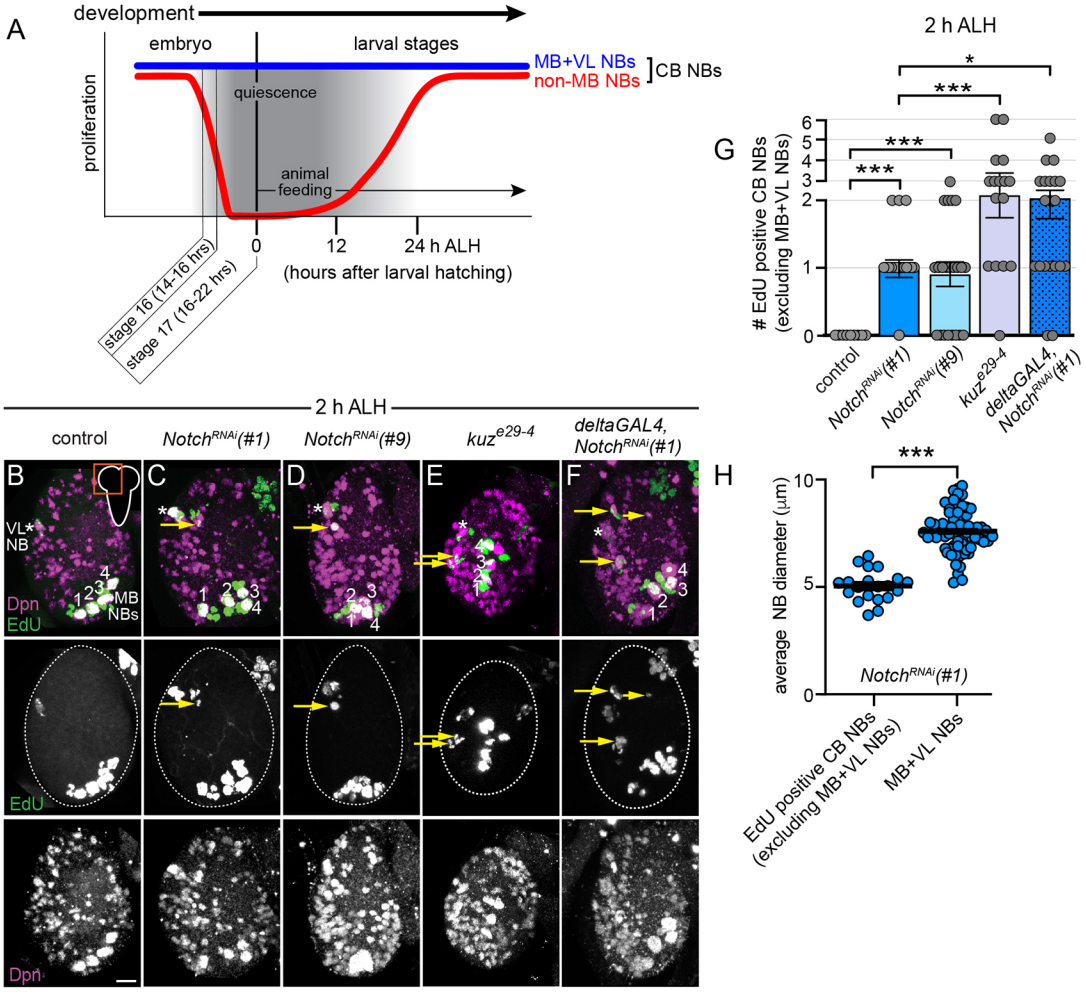

Fig. 1. Notch signaling positively regulates CB NB quiescence. (A) Schematic of late embryonic and early larval development showing CB NB proliferation patterns at indicated times. (B-F) Maximum intensity projections of single brain hemispheres from indicated genotypes at 2 h ALH showing EdU incorporation after 2 h of EdU treatment. Top panels are colored overlays with single channel grayscale images below. Numbers 1-4 indicate the MB NBs; the white asterisk indicates the VL NB and the yellow arrows indicate ectopic EdU incorporation in CB NBs. (G) Quantification of EdU-positive CB NBs (excluding MB+VL NBs) in the indicated genotypes after 2 h of larval EdU treatment. Each data point represents one brain hemisphere. Mean±s.e.m. ***$P\leq0.001$, *$P\leq0.033$ (Ordinary one-way ANOVA). (H) NB size (circle) after 2 h of larval EdU treatment in *Notch RNAi* animals, n=8 animals. Each data point represents one NB. Mean±s.e.m. ***$P\leq0.001$ (unpaired two-tailed Student's t-test). Scale bar: 10 µm. See Table S2 for panel genotypes.

Development (2022) 149, dev200275. doi:10.1242/dev.200275

NB (designated with an asterisk) (Fig. 1A; Fig. S1A-C) (Ito and Hotta, 1992; Truman and Bate, 1988; Britton and Edgar, 1998; Sousa-Nunes et al., 2011; Lin et al., 2013; Ding et al., 2016; Yuan et al., 2020). At this time, the MB and VL NBs are larger than quiescent CB NBs and are actively dividing based on expression of the S-phase indicator *pcna:GFP*, incorporation of the thymidine analogue EdU and their generation of EdU-positive progeny (Fig. S1A-C).

To determine whether Notch signaling regulates CB NB quiescence, we used GAL4/UAS to express *UAS-RNAi* transgenes targeted to Notch pathway components in NBs (*worGAL4*). In *NotchRNAi* animals, in addition to the MB+VL NBs, we observed on average one, occasionally two, Deadpan (Dpn)-positive CB NBs that incorporated EdU after 2 h of animal feeding, as well as more CB NBs expressing *pcna:GFP* compared with controls (Fig. 1B,C,G; Fig. S1D-F). We used a second RNAi line targeted against a different Notch exon and observed a similar phenotype (Fig. 1D,G). Unlike MB+VL NBs, the ectopic EdU positive CB NBs in *NotchRNAi* animals were small, similar in size to other quiescent CB NBs (Fig. 1H). Next, we assayed *kuzRNAi*, *neuralizedRNAi* and *Su(H)RNAi* animals and, again, found small ectopically proliferating EdU-positive CB NBs (Fig. S1G-J). To further substantiate whether Notch signaling regulates quiescence, we assayed the loss-of-function mutant allele, $kuz^{e29\text{-}4}$. In $kuz^{e29\text{-}4}$ homozygous animals, a modest, but significant, increase in the number of EdU-positive CB NBs was found compared with *NotchRNAi* animals (Fig. 1E,G). The number of Dpn-positive CB NBs was the same in $kuz^{e29\text{-}4}$ mutants as in controls (108.1±3.027 per brain hemisphere, n=6 animals; mean±s.e.m.), consistent with previous reports (Ulvklo et al., 2012; Bivik et al., 2016). Next, we used *DeltaGAL4* to increase expression levels of *UAS-RNAi* transgenes. Likewise, we found an increase in the number of

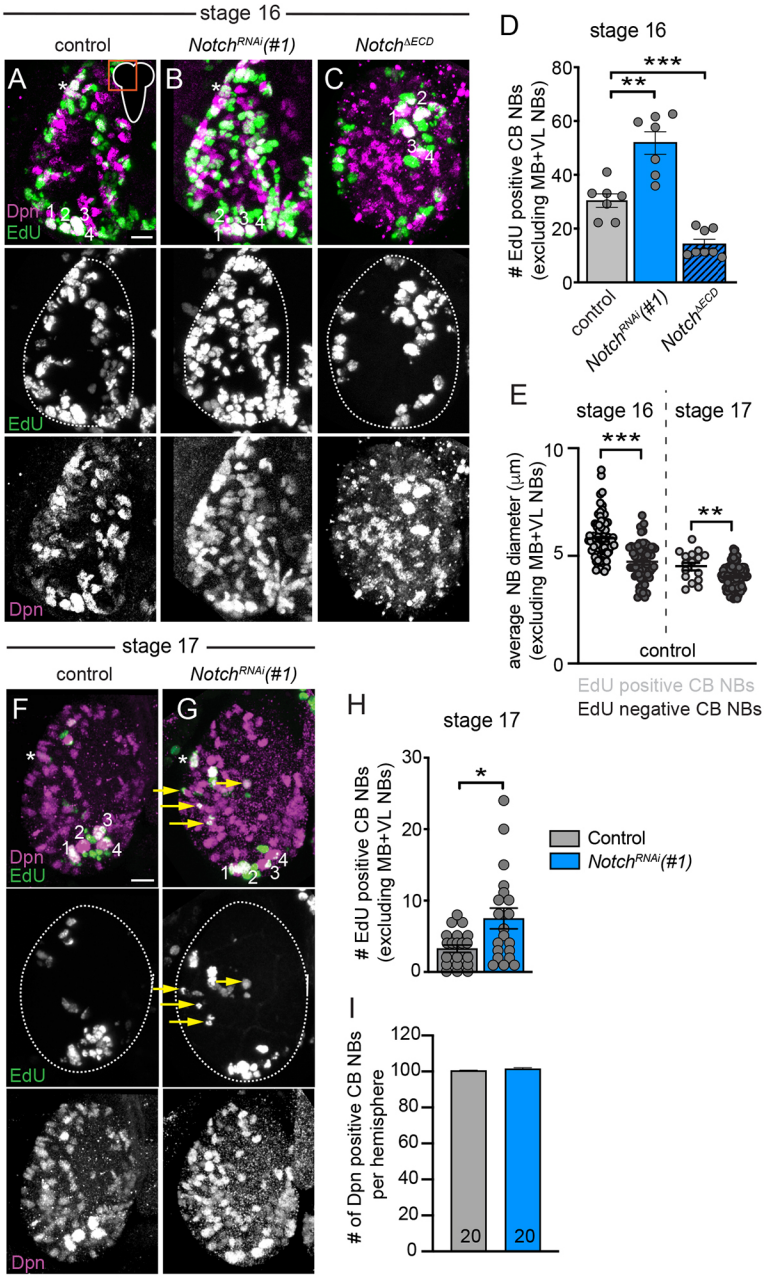

Fig. 2. Notch signaling regulates timing of quiescence entry. (A-C,F,G) Maximum intensity projections of single brain hemispheres from indicated genotypes and time points showing EdU incorporation after 1 h of EdU treatment. Top panels are colored overlays with single channel grayscale images below. Numbers 1-4 indicate the MB NBs; the white asterisk indicates the VL NB and the yellow arrows indicate ectopic EdU incorporation in CB NBs. (D,H) Quantification of EdU-positive CB NBs (excluding MB+VL NBs) in the indicated genotypes and time points after 1 h of larval EdU treatment. Each data point represents one brain hemisphere. Mean±s.e.m. ***P≤0.001, **P≤0.002, *P≤0.033 (unpaired two-tailed Student's t-test). (E) Quantification of EdU-positive versus EdU-negative CB NB size at the indicated time points. Each data point represents one NB from n=3 animals. Mean ±s.e.m. ***P≤0.00, **P≤0.002 (unpaired two-tailed Student's t-test). (I) Quantification of total number of Dpn-expressing CB NBs for the indicated genotypes at embryonic stage 17. Data represent mean±s.e.m. from n=10 animals, 20 brain hemispheres. Scale bars: 10 µm. See Table S2 for panel genotypes.

Development (2022) 149, dev200275. doi:10.1242/dev.200275

EdU-positive CB NBs compared with *worGAL4,UAS-NotchRNAi* animals (Fig. 1F,G). To confirm that *DeltaGAL4* increased *NotchRNAi* expression levels resulting in better knockdown of Notch signaling, we assayed expression of the Notch activity reporter *E(spl)mγ-GFP* (Almeida and Bray, 2005). Compared with controls, *E(spl)mγ-GFP* reporter expression was reduced in CB NBs in *worGAL4,UAS-NotchRNAi* animals and even further reduced in *DeltaGAL4,UAS-NotchRNAi* (Fig. S1K-M). We conclude that Notch pathway activity positively regulates CB NB quiescence.

Notch signaling positively regulates timing of quiescence entry

Next, we assayed earlier developmental time points to determine whether Notch signaling promotes quiescence entry or is required to maintain the quiescent state. In controls at embryonic stage 16, ∼30 CB NBs on average (excluding MB+VL NBs) incorporated EdU after 1 h treatment and, at stage 17, ∼3 CB NBs (Fig. 2A,D,F,H). At both stages, EdU-positive CB NBs were larger than EdU-negative CB NBs, yet the size difference was less at stage 17 (Fig. 2E). This suggests that CB NBs, as a population, complete their final reductive divisions between embryonic stages 16 and 17. In *Notch RNAi* animals at embryonic stages 16 and 17, we found more CB NBs that were proliferating based on EdU incorporation and *pcna:GFP* expression (Fig. 2B,D,G,H; Fig. S2A-C). We assayed total CB NB number in each of the brain hemispheres as well as CB NB size and found no differences in *Notch RNAi* animals compared with controls (Fig. 2I; Fig. S2D). This suggests that Notch signaling regulates CB NB entry into quiescence and when Notch pathway activity is reduced quiescence is delayed. To further test this possibility, we expressed a constitutively active form of the Notch receptor ($Notch^{\Delta ECD}$) in CB NBs (Vaccari et al., 2008). In

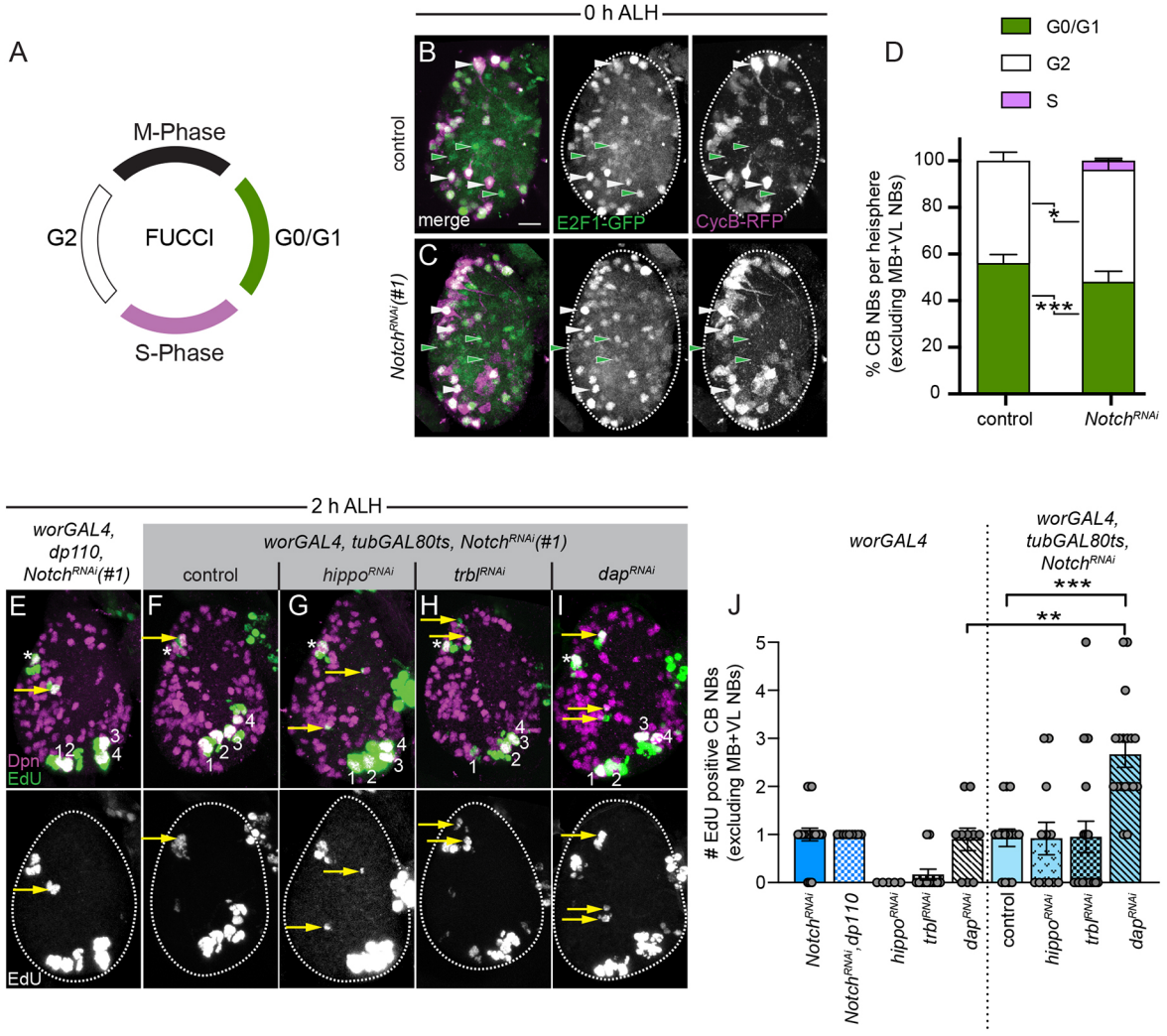

Fig. 3. Notch signaling promotes quiescence by inhibiting CB NB cell cycle progression. (A) Schematic of FUCCI labeling during cell cycle. (B,C) Maximum intensity projections of single brain hemispheres from indicated genotypes at 0 h ALH. Panels to the left are colored overlays with single channel grayscale images to the right. Green arrowheads indicate G0/G1-arrested CB NBs and white arrowheads indicate G2-arrested CB NBs (D) Quantification of cell cycle state of the CB NBs (excluding MB+VL NBs) from indicated genotypes at 0 h ALH. Data represent mean+s.e.m. from n=3 animals. ***P≤0.001, *P≤0.033 (unpaired two-tailed Student's t-test using Holm-Sidak correction). (E-I) Maximum intensity projections of single brain hemispheres from indicated genotypes at 2 h ALH showing EdU incorporation after 2 h of EdU treatment. Top panels are colored overlays with single channel grayscale image below. Numbers 1-4 indicate the MB NBs; the white asterisk indicates the VL NB and the yellow arrows indicate ectopic EdU incorporation in CB NBs. (J) Quantification of EdU-positive CB NBs (excluding MB+VL NBs) in the indicated genotypes after 2 h of larval EdU treatment. Each data point represents one brain hemisphere. Mean±s.e.m. ***P≤0.001, **P≤0.002 (Kolmogorov–Smirnov test). Scale bar: 10 µm. See Table S2 for panel genotypes.

Development (2022) 149, dev200275. doi:10.1242/dev.200275

Notch^{AECD} animals at embryonic stage 16, we found a reduction in the number of proliferating CB NBs compared with controls (Fig. 2C,D). We conclude that Notch pathway activity positively regulates timing of quiescence entry.

Notch signaling promotes quiescence by inhibiting CB NB cell cycle progression

Next, we asked whether Notch signaling promotes quiescence by inhibiting CB NB cell cycle progression or by regulating temporal patterning. First, we used fluorescent ubiquitination-based cell cycle indicator (FUCCI) to determine cell cycle states of quiescent CB NBs (Zielke et al., 2014; Otsuki and Brand, 2018). In control animals at the freshly hatched larval stage (0 h ALH), more than half of quiescent CB NBs were G0/G1-arrested and the rest were G2-arrested (Fig. 3A,B,D). In contrast, in *Notch RNAi* animals, less than half were G0/G1-arrested and the rest were G2-arrested or actively dividing (Fig. 3C,D). This suggests that Notch signaling inhibits CB NB cell cycle progression. Next, we co-expressed a number of UAS-transgenes to manipulate CB NB cell cycle and/or growth in *NotchRNAi* animals, including *UAS-dp110*, the catalytic subunit of PI3-kinase, *UAS-hippoRNAi*, *UAS-trblRNAi* and *UAS-dacapoRNAi*. These transgenes were selected because they all affect genes and/or cell signaling pathways implicated previously in quiescence, entry and exit, and they all regulate aspects of NB cell cycle and growth (Leevers et al., 1996; Ding et al., 2016; Otsuki and Brand, 2018, 2019). We found a significant increase in the number of EdU-positive NBs in *NotchRNAi*, *dacapoRNAi* animals compared with animals expressing either *NotchRNAi* or *dacapoRNAi* alone (Fig. 3F,I,J). No differences were detected following co-expression of other transgenes (Fig. 3E-J). Next, to distinguish whether Notch promotes quiescence by regulating temporal patterning, we assayed expression of the late temporal factor, Cas. We found no difference in the number of Cas-positive CB NBs in control animals compared with *NotchRNAi* animals, consistent with previous reports (Fig. S2E; Ulvklo et al., 2012; Chang et al., 2013). Together, these results support that Notch signaling promotes quiescence by regulating activity of the cell cycle exit gene, *dap*, a known Notch target.

Notch signaling is active in proliferating, but not quiescent, CB NBs

Next, to better understand how Notch controls quiescence, we used *E(spl)mγ-GFP* to assay Notch pathway activity (Almeida and Bray, 2005). At embryonic stage 16, *E(spl)mγ-GFP* reporter expression was detected in 90% of CB NBs, whereas at stage 17, 10% of CB NBs, and at 0 h ALH, 6% of CB NBs, retained expression of *E(spl)mγ-GFP* (Fig. 4A-C) (Zacharioudaki et al., 2012). Next, we assayed *E(spl)mγ-GFP* expression in MB+VL NBs, which divide

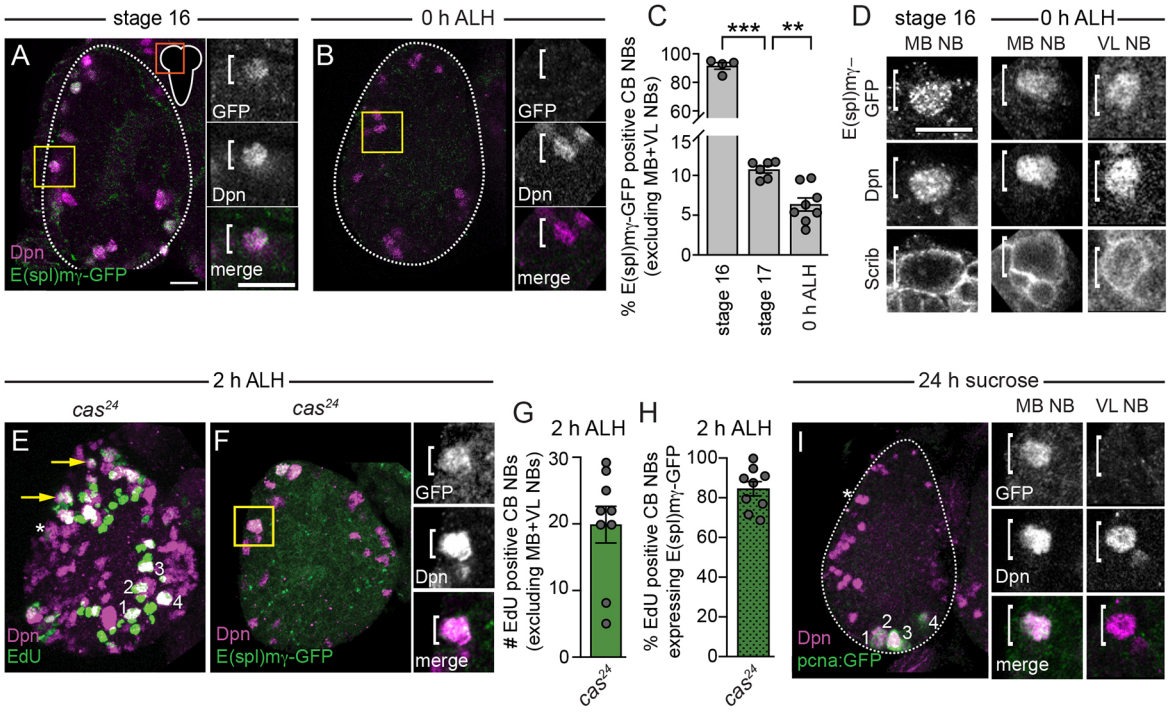

Fig. 4. Notch signaling is active in proliferating, but not quiescent CB NBs. (A,B,F) Single optical section of a brain hemisphere from indicated genotypes and time points showing expression of E(spl)mγ-GFP. Higher magnification images of the CB NBs highlighted by the yellow box are shown to the right of the colored overlays. White brackets indicate the neuroblast. Top panels are higher magnification single channel grayscale images with colored overlays below. (C) Quantification of the percentage of CB NBs (excluding MB+VL NBs) expressing *E(spl)mγ-GFP* at the indicated time points. Each data point represents one brain hemisphere. Mean±s.e.m. ***$P\leq0.001$, **$P\leq0.002$ (Brown-Forsythe and Welch ANOVA test). (D) Single optical section of wild-type MB NB and the VL NB from indicated time points showing expression of E(spl)mγ-GFP. White brackets indicate the neuroblast. (E,I) Maximum intensity projections of single brain hemisphere from indicated genotypes and time points showing EdU incorporation after 2 h of EdU treatment (E) and *pcna:GFP* expression (I). Numbers 1-4 indicate the MB NBs; the white asterisk indicates the VL NB and the yellow arrows indicate ectopic EdU incorporation in CB NBs. Higher magnification images of the MB NB and the VL NB are shown to the right of the colored overlays. White brackets indicate the neuroblast. Top panels are higher magnification single channel grayscale images with colored overlays below (I). (G) Quantification of EdU-positive CB NBs (excluding MB+VL NBs) in 2 h ALH *cas*^{24} animals after 2 h of larval EdU treatment. Each data point represents one brain hemisphere. Mean±s.e.m. (H) Quantification of the percent of EdU-positive CB NBs (excluding MB+VL NBs) expressing *E(spl)mγ-GFP* in 2 h ALH *cas*^{24} animals. Each data point represents one brain hemisphere. Mean±s.e.m. Scale bars: 10 µm. See Table S2 for panel genotypes.

Development (2022) 149, dev200275. doi:10.1242/dev.200275

continuously during the embryonic-to-larval transition. We found *E(spl)mγ-GFP* reporter expression in MB+VL NBs at these stages (Fig. 4D). This suggests that Notch signaling is active in proliferating, but not in quiescent, CB NBs. To test this possibility, we assayed *E(spl)mγ-GFP* reporter expression in *cas* mutants. Cas positively regulates quiescence in ventral nerve cord NBs by inhibiting expression of the early temporal factor Pdm (Kambadur et al., 1998; Tsuji et al., 2008). Consistent with previous reports (Tsuji et al., 2008), we found a significant number of EdU-positive CB NBs in brains of *cas* homozygous mutants compared with controls (Fig. 4E,G), the majority of which expressed *E(spl)mγ-GFP* (Fig. 4F,H). Next, we fed freshly hatched *pcna:GFP* larvae a sucrose-only diet. After 24 h of animal feeding, MB NBs continued dividing and expressed *E(spl)mγ-GFP* (Fig. 4I). In contrast, the VL NB stopped and *E(spl)mγ-GFP* reporter expression was not detected (Fig. 4I). Lastly, we blocked CB NB mitosis and division by knocking down the cdc25 phosphatase, *string*, in NBs. At embryonic stage 16, we found an equal number of EdU-positive CB NBs compared with controls, but a strong reduction in the number of EdU-positive CB NB progeny, consistent with G2-arrest (Fig. S3A,B). Compared with controls, *stringRNAi* animals had a strong reduction in CB NBs expressing the *E(spl)mγ-GFP* reporter (Fig. S3C-E). We conclude that Notch signaling is active in proliferating NBs, but not in NBs that are in quiescence or those that have exited the cell cycle.

To better understand how Notch activity is regulated during the embryonic-to-larval transition and to understand how Notch pathway activity becomes attenuated, we assayed expression and localization of the Notch receptor and the Notch ligands, Delta and Serrate. We assayed expression in both MB+VL NBs, which maintain Notch activity and continue dividing, and in the other CB NBs, which stop dividing and have low to no Notch activity. At embryonic stage 16 and in freshly hatched larvae at 0 h ALH, Notch was expressed in CB NBs, including MB+VL NBs (Fig. 5A; Fig. S4A). At embryonic stage 16, Delta was also expressed in CB NBs, including MB+VL NBs, but by 0 h ALH Delta was reduced in quiescent CB NBs compared with MB+VL NBs (Fig. 5B,C; Fig. S4B). This is similar to *E(spl)mγ-GFP* reporter expression (Fig. 4C), suggesting that decreases in Delta could account for Notch pathway attenuation. Next, we fed freshly hatched larvae (0 h ALH) a complete diet to reactivate quiescent CB NBs. Reactivated CB NBs expressed both Notch and Delta and had active Notch signaling based on *E(spl)mγ-GFP* reporter expression (Fig. S4C-H). In addition, we observed Delta in newborn GMCs, adjacent to their CB NB mothers (Fig. 5B; Fig. S4F, yellow bracket). Serrate was not detected at any of these time points (Fig. S4I,J). Together, we conclude that Notch signaling is required for quiescence, but that Notch is not active in quiescent CB NBs. Moreover, proliferating CB NBs, but not quiescent, generate Delta-expressing GMCs.

Expression of Delta in GMCs adjacent to proliferating NBs suggests that GMC-localized Delta transactivates Notch in NBs. To further examine this possibility, we fed freshly hatched animals a complete diet for 12 h to visualize the first CB NB S-phase and cell division after quiescence (Fig. 5D,E). At 12 h after feeding before S-phase entry, Delta levels were increased in CB NBs compared with CB NBs at 0 h ALH (Fig. 5D). Delta was localized symmetrically in mitotic NBs and, after division, Delta-expressing GMCs were found adjacent to their NB mothers (Fig. 5D,F). Coinciding with the production of Delta-expressing GMCs, CB

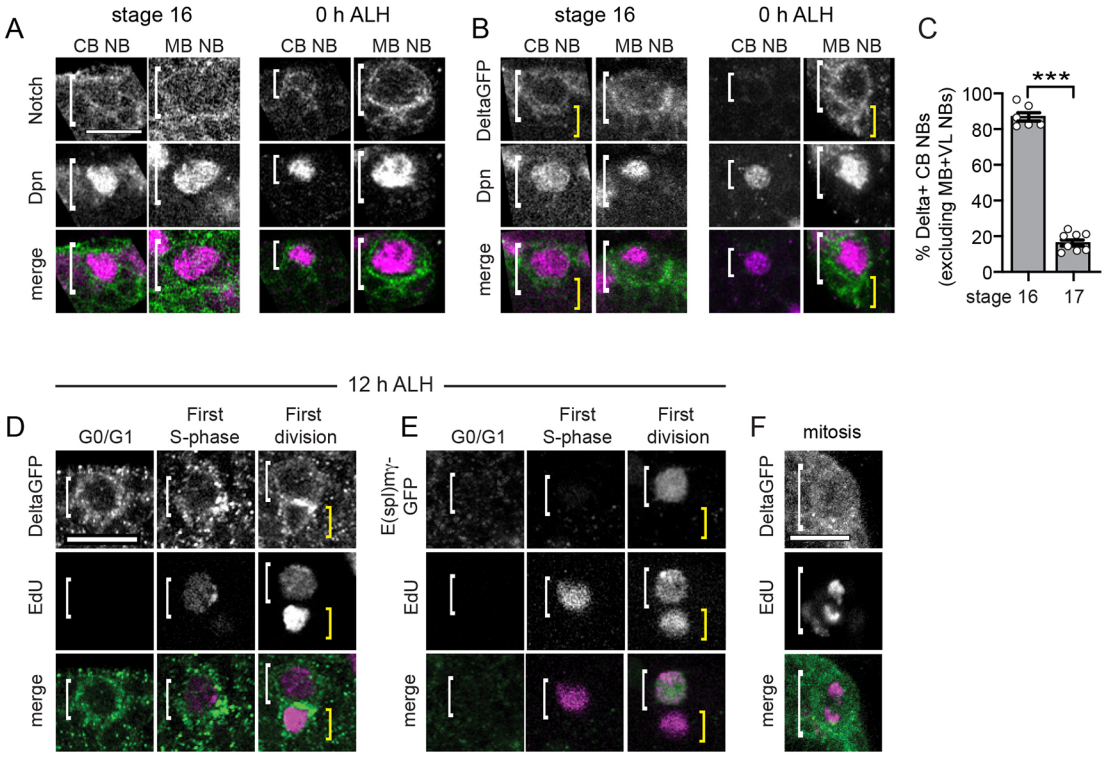

Fig. 5. Delta is expressed in CB NBs and inherited by daughter cells post NB division to activate Notch signaling in proliferating CB NBs. (A,B,D-F) Single optical section of wild-type CB NBs and MB NBs showing expression of Notch ICD antibody (A), *DeltaGFP* (B,D,F) and *E(spl)mγ-GFP* (E) at the indicated time points. White brackets indicate the neuroblast and the yellow brackets indicate the newborn GMCs. Top panels are single channel grayscale images with the colored overlay below. (C) Quantification of the percentage of CB NBs (excluding MB+VL NBs) expressing *DeltaGFP* at indicated time points. Each data point represents one brain hemisphere. Mean±s.e.m. ***$P \leq 0.001$ (unpaired two-tailed Student's *t*-test). Scale bars: 10 µm. See Table S2 for panel genotypes.

Development (2022) 149, dev200275. doi:10.1242/dev.200275

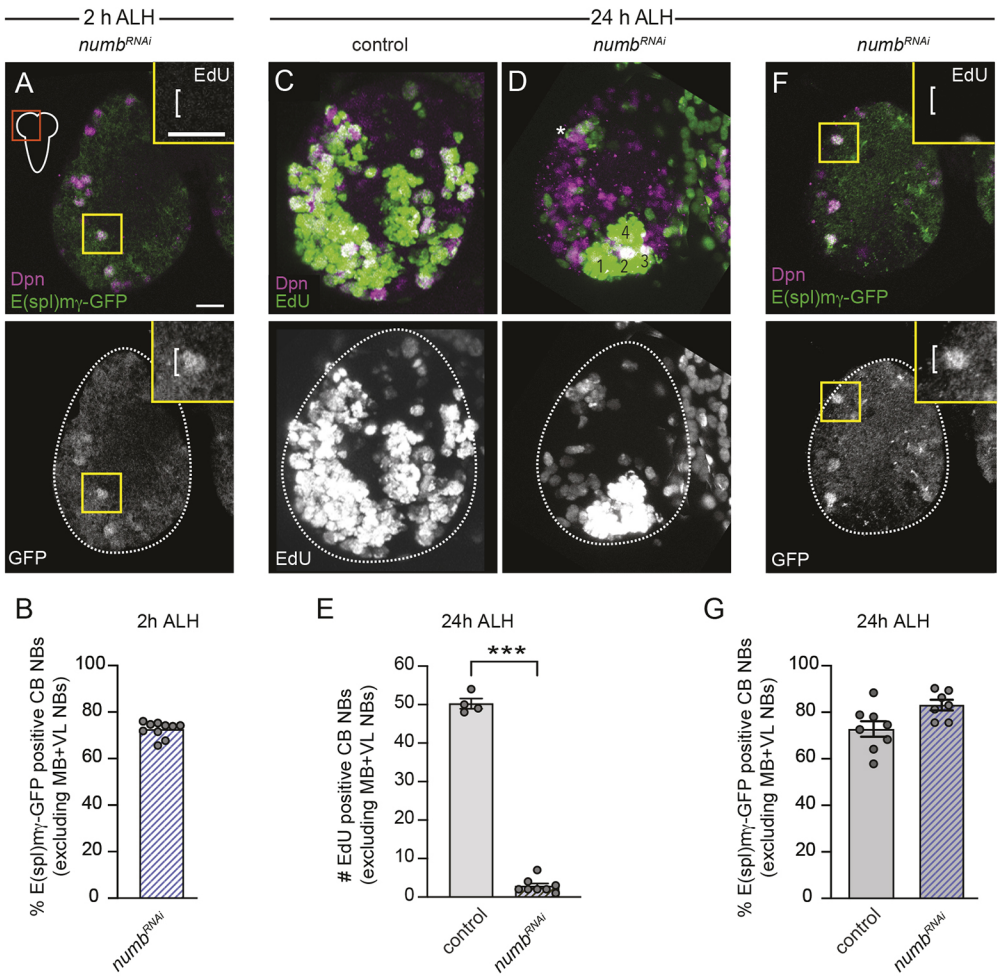

Fig. 6. Low Notch is required for quiescent CB NBs to reactivate in response to dietary nutrients. (A,F) Single optical section of a brain hemisphere from *numb* knockdown animals at indicated time points showing expression of E(spl)mγ-GFP. Top panels are colored overlays with single channel grayscale image below. Insets show higher magnification image of the highlighted (yellow box) CB NBs. White brackets indicate the neuroblast. (B,G) Quantification of the percentage of CB NBs (excluding MB+VL NBs) expressing *E(spl)mγ-GFP* from indicated genotypes and time points. Each data point represents one brain hemisphere. Mean±s.e.m. (C,D) Maximum intensity projections of single brain hemispheres from indicated genotypes at 24 h ALH showing EdU incorporation after 24 h of EdU treatment. Top panels are colored overlays with single channel grayscale image below. Numbers 1-4 indicate the MB NBs and the white asterisk indicates the VL NB. (E) Quantification of EdU-positive CB NBs (excluding MB+VL NBs) in the indicated genotypes and time points after 24 h of larval EdU treatment. Each data point represents one brain hemisphere. Mean±s.e.m. ***$P \leq 0.001$ (unpaired two-tailed Student's *t*-test). Scale bar: 10 µm. See Table S2 for panel genotypes.

NBs expressed *E(spl)mγ-GFP* (Fig. 5E) (Zacharioudaki et al., 2012). We conclude that NBs generate their own ligand-expressing daughters for Notch pathway transactivation and because CB NBs exit cell cycle, Notch activity becomes attenuated.

Low Notch is required for quiescent CB NBs to reactivate in response to dietary nutrients

To determine whether inactivation of Notch signaling is important for quiescence or is simply a consequence of NB cell cycle exit and quiescence entry, we expressed *UAS-numbRNAi* in NBs to activate Notch signaling. Numb inhibits Notch signaling and, in *numbRNAi* animals, we found *E(spl)mγ-GFP* reporter expression in quiescent CB NBs at 0 h ALH, consistent with Notch pathway activation (Fig. 6A,B). Next, we fed *numbRNAi* animals a complete diet. After 24 h of feeding, most CB NBs in control animals had reactivated from quiescence based on their increased size, expression of *pcna:GFP*, incorporation of EdU and generation of EdU-positive progeny (Fig. 6C,E) (Sousa-Nunes et al., 2011; Lin et al., 2013; Sipe and Siegrist, 2017; Yuan et al., 2020). In contrast, in *numbRNAi* animals, few CB NBs incorporated EdU after 24 h of animal feeding, yet *E(spl)mγ-GFP* reporter expression was still maintained (Fig. 6D-G). We conclude that inactivation of Notch signaling is required for CB NBs to reactivate in response to dietary nutrients.

Notch activity increases in late-stage embryonic CB NBs

Although Notch is active in CB NBs throughout most of embryogenesis, Notch induces quiescence only at late stages. This suggests that Notch activity or Notch targets change over time. To assay Notch activity, we examined the subcellular localization of Notch ICD. We found a modest, but significant, increase in nuclear localized Notch ICD in stage 16 CB NBs compared with stage 10 (Fig. 7A), consistent with other studies (Ulvklo et al., 2012). Next, we asked whether temporal patterning restricts Notch function to late stages. In *nubbin/pdm2* mutant wing discs, Notch target genes are ectopically expressed, and in *nubbin/pdm2* mutants, ventral cord NBs enter quiescence prematurely (Neumann and Cohen, 1998; Tsuji et al., 2008). Because of technical constraints, we were unable to reduce Notch pathway components in *nubbin/pdm2* mutants. However, we did assay quiescence in *cas* mutants following constitutive activation of Notch signaling. Compared with *cas* mutants alone, we found no difference in the number of EdU-positive CB NBs (Fig. 7B). These results suggest that temporal factor patterning provides Notch signaling competence to induce CB NB cell cycle exit and quiescence, either by regulating Notch activity levels or by regulating Notch targets.

DISCUSSION

Here, we report that Notch signaling regulates quiescence, entry and exit in *Drosophila* CB NBs (model Fig. 7C). Increasing Notch pathway activity induces CB NBs to exit cell cycle via a Dap-dependent mechanism. Dap, a cyclin-dependent kinase inhibitor and CIP/KIP family member, is a known Notch target gene as is Cyclin E, String (Cdc25) and E2F (Sriuranpong et al., 2001; Deng et al., 2001; Noseda et al., 2004; Herranz et al., 2008; Ishikawa et al., 2008;

Development (2022) 149, dev200275. doi:10.1242/dev.200275

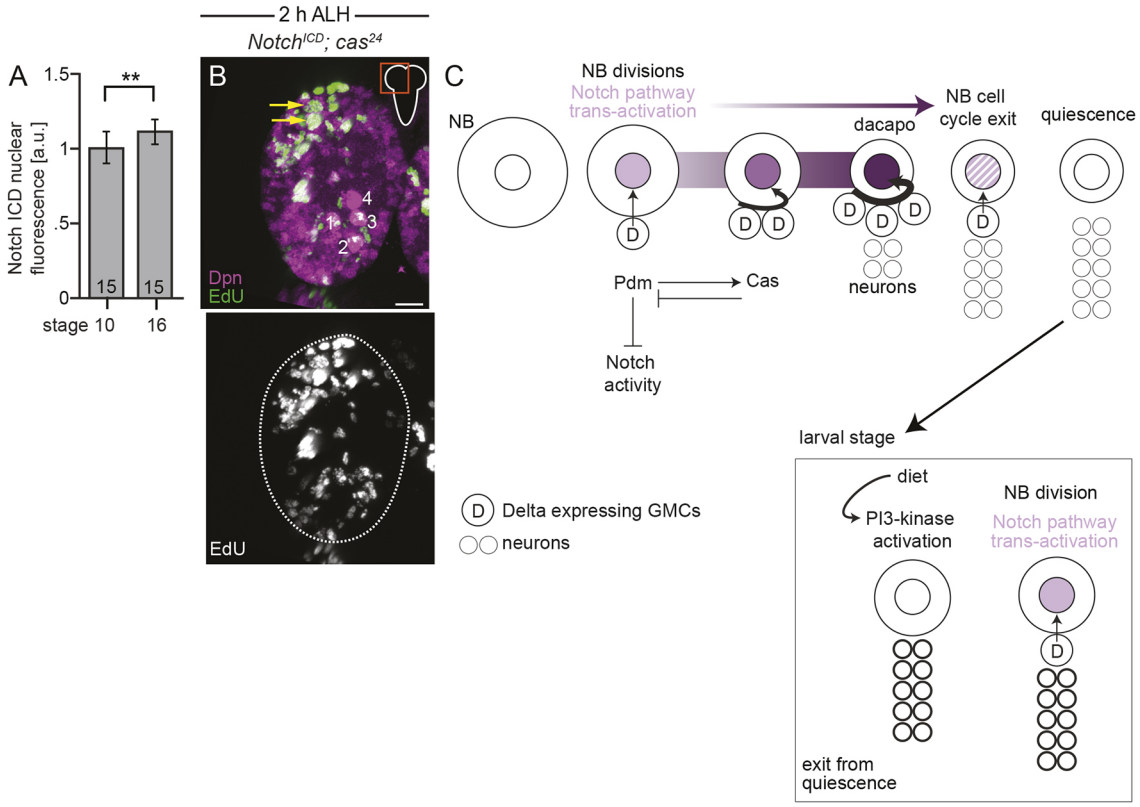

Fig. 7. Notch activity increases in late-staged embryonic CB NBs. (A) Normalized Notch ICD nuclear fluorescence intensities in wild-type CB NBs at indicated time points. Column numbers indicate number of CB NBs assayed, error bars show s.e.m., $^{**}P \leq 0.002$ (unpaired two-tailed Student's *t*-test). (B) Maximum intensity projections of single brain hemispheres from indicated genotypes at 2 h ALH showing EdU incorporation after 2 h of EdU treatment. Top panel is colored overlay with single channel grayscale image below. Numbers 1-4 indicate the MB NBs and the yellow arrows indicate ectopic EdU incorporation in CB NBs. (C) Model summary. Notch pathway is activated in the NBs by its adjacent Delta-expressing daughter cells. Over time, in response to NB intrinsic temporal cues and an increase in the number of daughter cells produced, Notch activity in the NBs increases to promote expression of Dap and consequent exit from cell cycle. As the daughter cells differentiate they lose expression of Delta and the Notch pathway is turned off in the quiescent NBs. Later, upon PI3-K activation the NBs reactivate and divide to produce Delta-expressing daughter cells to once again activate the Notch pathway in the NBs. Scale bar: 10 µm. See Table S2 for panel genotypes.

Bivik et al., 2016; Shang et al., 2016). Whether Notch regulates other cell cycle genes required for CB NB exit remains unknown. Once CB NBs stop dividing, Notch pathway activity becomes attenuated. Low to no Notch activity is required for CB NBs to exit quiescence in response to dietary nutrient cues. Thus, levels of CB NB Notch activity regulate both the entry and exit from quiescence. High Notch is required for entry, whereas low Notch is required for exit. Intestinal stem cells (ISCs) also experience a period of low to no Notch activity during mid-pupal stages and, if Notch is ectopically induced at this time, ISCs terminally differentiate into secretory enteroendocrine cells (Guo and Ohlstein, 2015). Whether any of the quiescent CB NBs with ectopic Notch terminally differentiate remains unknown.

Although Notch is required for quiescence, most CB NBs do stop dividing, albeit late. This suggests that other genes or signaling pathways are required or that residual Notch activity is sufficient to induce CB NB quiescence. Unfortunately, Notch null mutants are embryonic lethal (Lehmann et al., 1983; Parody and Muskavitch, 1993; Brennan et al., 1997; Leonardi et al., 2011). In addition, we have shown that Notch is sufficient to induce quiescence. Although quiescence occurs prematurely, it is still restricted to late embryonic stages. Restriction of Notch function (cell cycle exit) is likely due to CB NB intrinsic temporal programs. Temporal programs that likely vary across CB NB lineages, as is the case in the ventral nerve cord. Whether temporal programs regulate levels of Notch pathway activity or provide additional factors needed for CB NB cell cycle exit remains unanswered.

In mammals, Notch signaling is more complicated because of gene duplication. Yet, recently, Notch signaling has been shown to regulate neural stem cell quiescence. In *Notch2* conditional knockout mice, more neural stem cells are actively dividing in the hippocampus and subventricular zone brain regions in adult animals compared with controls (Engler et al., 2018; Zhang et al., 2019). This results in premature depletion of the neural stem pool and reduced neurogenesis in older mice (Engler et al., 2018; Zhang et al., 2019). This is similar to what we report here and, in the future, it will be interesting to determine which Notch ligands are required and whether neural stem cells in mammals use their newborn daughters for pathway activation.

MATERIALS AND METHODS

Fly stocks

Fly stocks used in this study and their source are listed in Table S1.

Embryo collections and animal husbandry

Embryos were collected for 0-2 h or 0-4 h after egg laying (AEL) and aged for 13-22 h at 25°C. For experiments using *tub-Gal80ts* (temperature sensitive), embryos and larvae were kept at 29°C. For larval staging, animals were collected immediately after hatching and transferred to either standard Bloomington fly food or 20% sucrose-only solution for the desired amount of time. For embryonic staging, embryos were aged at 25°C for 13-15 h AEL to get stage 16 embryos and for 16-20 h AEL to get stage 17 embryos. For genotypes (kuz^{e29-4} and cas^{24}) where embryos failed to hatch, embryos were dechorionated and dissected (Lee et al., 2009) at 24 h AEL to get larvae.

Development (2022) 149, dev200275. doi:10.1242/dev.200275

EdU incorporation assay

For EdU incorporation assays, Bloomington fly food or Schneider's insect media was supplemented with 0.2 mM EdU. For larval EdU incorporation experiments, freshly hatched larvae were transferred to EdU food for 2 h at 25°C. For embryonic EdU incorporation experiments, embryos were dechorionated and dissected (Lee et al., 2009). Dissected embryonic tissue was transferred to Schneider's insect media supplemented with EdU for 60 min at room temperature. EdU incorporation was detected using the Click-iT EdU Proliferation Kit for Imaging and Alexa Fluor 647 dye (Thermo Fisher Scientific, C10340) as described previously (Sipe and Siegrist, 2017; Yuan et al., 2020).

Immunofluorescence and confocal imaging

Embryonic and larval brains were dissected as described previously (Sipe and Siegrist, 2017; Yuan et al., 2020). In brief, dissected tissues were fixed in 4% EM-grade formaldehyde in PEM buffer for 20 min and rinsed in 1× PBS with 0.1% Triton X-100 (PBT). Tissues were blocked overnight at 4°C in 10% normal goat serum in PBT followed by antibody staining. Primary antibodies used include chicken anti-GFP (1:500, Abcam, ab13970), rat anti-Deadpan (Dpn, 1:100, Abcam, ab195173), mouse anti-Notch ICD (1:250; Developmental Studies Hybridoma Bank, C17.9C6), rabbit anti-dsRed (1:1000; Clontech, 632496) and rabbit anti-Scribble (Scrib, 1:1000, gift from Chris Q. Doe, University of Oregon, OR, USA). To detect primary antibodies, the following Alexa-Fluor conjugated secondary antibodies were used: goat anti-chicken Alexa 488 (1:300; A32931), goat anti-mouse Alexa 488 (1:300, A11001), goat anti-rat Alexa 555 (1:300, A48263), goat anti-rabbit Alexa 555 (1:300, A21428) and goat anti-rabbit Alexa 633 (1:300, A21071) (Thermo Fisher Scientific).

Images encompassing the entire brain hemispheres were acquired using a Leica SP8 laser scanning confocal microscope equipped with a 63×/1.4 NA oil-immersion objective and analyzed using Fiji software. All images were processed using Fiji and Adobe Photoshop and figures were assembled using Adobe Illustrator. NBs were identified based on Dpn expression and superficial location. The Fiji 'cell counter' plugin was used to count and track the number of EdU- and/or GFP-expressing Dpn-positive NBs. NB size was calculated by averaging the lengths of two perpendicular lines through the center of the NB in Fiji.

Quantification of fluorescence was performed in Fiji. Cytoplasmic and nuclear Notch ICD levels were quantified as follows. NBs labeled with Scribble and nuclei labeled with Dpn were manually traced and the average Notch ICD fluorescence intensity measured in the whole cell and the nucleus using Fiji. Notch ICD nuclear fluorescence intensity was determined as a ratio of nuclear Notch ICD fluorescence intensity to whole cell Notch ICD fluorescence intensity.

All data is represented as mean±s.e.m. and statistical significance was determined using unpaired two-tailed Student's *t*-tests or ANOVAs in Prism 9.

Acknowledgements

We thank Cheng-Yu Lee for providing fly stocks. We thank the Bloomington Drosophila Stock Center, Harvard TRiP and the Developmental Studies Hybridoma Bank for providing flies and antibody reagents. We especially thank Siegrist Lab members, Md Ausrafuggaman Nahid, and Karsten Siller for providing comments on the manuscript.

Competing interests

The authors declare no competing or financial interests.

Author contributions

Conceptualization: C.S.; Methodology: C.S., V.T.J., S.E.D.; Validation: C.S.; Formal analysis: C.S.; Investigation: C.S., V.T.J., S.E.D., S.E.S.; Resources: C.S.; Data curation: C.S.; Writing - original draft: C.S., S.E.S.; Writing - review & editing: C.S., S.E.D., S.E.S.; Visualization: C.S.; Supervision: S.E.S.; Project administration: S.E.S.; Funding acquisition: S.E.S.

Funding

This work was funded by National Institutes of Health/National Institute of General Medical Sciences (R01-GM120421). Deposited in PMC for release after 12 months.

Peer review history

The peer review history is available online at https://journals.biologists.com/dev/article-lookup/doi/10.1242/dev.200275.

References

Almeida, M. S. and Bray, S. J. (2005). Regulation of post-embryonic neuroblasts by Drosophila Grainyhead. *Mech. Dev.* **122**, 1282-1293. doi:10.1016/j.mod.2005.08.004

Bivik, C., MacDonald, R. B., Gunnar, E., Mazouni, K., Schweisguth, F. and Thor, S. (2016). Control of neural daughter cell proliferation by multi-level Notch/Su(H)/E(spl)-HLH signaling. *PLoS Genet.* **12**, e1005984. doi:10.1371/journal.pgen.1005984

Brennan, K., Tateson, R., Lewis, K. and Arias, A. M. (1997). A functional analysis of Notch mutations in Drosophila. *Genetics* **147**, 177-188. doi:10.1093/genetics/147.1.177

Britton, J. S. and Edgar, B. A. (1998). Environmental control of the cell cycle in Drosophila: nutrition activates mitotic and endoreplicative cells by distinct mechanisms. *Development* **125**, 2149-2158. doi:10.1242/dev.125.11.2149

Cavallucci, V., Fidaleo, M. and Pani, G. (2016). Neural stem cells and nutrients: poised between quiescence and exhaustion. *Trends Endocrinol. Metab.* **27**, 756-769. doi:10.1016/j.tem.2016.06.007

Chang, Y.-C., Jang, A. C.-C., Lin, C.-H. and Montell, D. J. (2013). Castor is required for Hedgehog-dependent cell-fate specification and follicle stem cell maintenance in Drosophila oogenesis. *Proc. Natl. Acad. Sci. USA* **110**, E1734-E1742. doi:10.1073/pnas.1300725110

Chell, J. M. and Brand, A. H. (2010). Nutrition-responsive glia control exit of neural stem cells from quiescence. *Cell* **143**, 1161-1173. doi:10.1016/j.cell.2010.12.007

Cheung, T. H. and Rando, T. A. (2013). Molecular regulation of stem cell quiescence. *Nat. Rev. Mol. Cell Biol.* **14**, 329-340. doi:10.1038/nrm3591

Cho, I. J., Lui, P. P. W., Obajdin, J., Riccio, F., Stroukov, W., Willis, T. L., Spagnoli, F. and Watt, F. M. (2019). Mechanisms, hallmarks, and implications of stem cell quiescence. *Stem Cell Rep.* **12**, 1190-1200. doi:10.1016/j.stemcr.2019.05.012

Choksi, S. P., Southall, T. D., Bossing, T., Edoff, K., de Wit, E., Fischer, B. E., van Steensel, B., Micklem, G. and Brand, A. H. (2006). Prospero acts as a binary switch between self-renewal and differentiation in Drosophila neural stem cells. *Dev. Cell* **11**, 775-789. doi:10.1016/j.devcel.2006.09.015

Coller, H. A. (2019). The paradox of metabolism in quiescent stem cells. *FEBS Lett.* **593**, 2817-2839. doi:10.1002/1873-3468.13608

Colonques, J., Ceron, J., Reichert, H. and Tejedor, F. J. (2011). A Transient expression of prospero promotes cell cycle exit of Drosophila postembryonic neurons through the regulation of Dacapo. *PLoS ONE* **6**, e19342. doi:10.1371/journal.pone.0019342

De Strooper, B., Annaert, W., Cupers, P., Saftig, P., Craessaerts, K., Mumm, J. S., Schroeter, E. H., Schrijvers, V., Wolfe, M. S., Ray, W. J. et al. (1999). A presenilin-1-dependent γ-secretase-like protease mediates release of Notch intracellular domain. *Nature* **398**, 518-522. doi:10.1038/19083

Deng, W.-M., Althauser, C. and Ruohola-Baker, H. (2001). Notch-Delta signaling induces a transition from mitotic cell cycle to endocycle in Drosophila follicle cells. *Development* **128**, 4737-4746. doi:10.1242/dev.128.23.4737

Ding, R., Weynans, K., Bossing, T., Barros, C. S. and Berger, C. (2016). The Hippo signalling pathway maintains quiescence in Drosophila neural stem cells. *Nat. Commun.* **7**, 10510. doi:10.1038/ncomms10510

Engler, A., Rolando, C., Giachino, C., Saotome, I., Erni, A., Brien, C., Zhang, R., Zimber-Strobl, U., Radtke, F., Artavanis-Tsakonas, S. et al. (2018). Notch2 signaling maintains NSC quiescence in the murine ventricular-subventricular zone. *Cell Rep.* **22**, 992-1002. doi:10.1016/j.celrep.2017.12.094

Fiuza, U.-M. and Arias, A. M. (2007). Cell and molecular biology of Notch. *J. Endocrinol.* **194**, 459-474. doi:10.1677/JOE-07-0242

Fortini, M. E. and Artavanis-Tsakonas, S. (1994). The suppressor of hairless protein participates in notch receptor signaling. *Cell* **79**, 273-282. doi:10.1016/0092-8674(94)90196-1

Guo, Z. and Ohlstein, B. (2015). Bidirectional Notch signaling regulates *Drosophila* intestinal stem cell multipotency. *Science* **350**, aab0988. doi:10.1126/science.aab0988

Herranz, H., Pérez, L., Martín, F. A. and Milán, M. (2008). A Wingless and Notch double–repression mechanism regulates G1–S transition in the Drosophila wing. *EMBO J.* **27**, 1633-1645. doi:10.1038/emboj.2008.84

Hirata, J., Nakagoshi, H., Nabeshima, Y.-I. and Matsuzaki, F. (1995). Asymmetric segregation of the homeodomain protein Prospero duringDrosophila development. *Nature* **377**, 627-630. doi:10.1038/377627a0

Homem, C. C. F., Steinmann, V., Burkard, T. R., Jais, A., Esterbauer, H. and Knoblich, J. A. (2014). Ecdysone and mediator change energy metabolism to terminate proliferation in Drosophila neural stem cells. *Cell* **158**, 874-888. doi:10.1016/j.cell.2014.06.024

Ishikawa, Y., Onoyama, I., Nakayama, K. I. and Nakayama, K. (2008). Notch-dependent cell cycle arrest and apoptosis in mouse embryonic fibroblasts lacking Fbxw7. *Oncogene* **27**, 6164-6174. doi:10.1038/onc.2008.216

Ito, K. and Hotta, Y. (1992). Proliferation pattern of postembryonic neuroblasts in the brain of Drosophila melanogaster. *Dev. Biol.* **149**, 134-148. doi:10.1016/0012-1606(92)90270-Q
Kalamakis, G., Brüne, D., Ravichandran, S., Bolz, J., Fan, W., Ziebell, F., Stiehl, T., Catalá-Martinez, F., Kupke, J., Zhao, S. et al. (2019). Quiescence modulates stem cell maintenance and regenerative capacity in the aging brain. *Cell* **176**, 1407-1419.e14. doi:10.1016/j.cell.2019.01.040
Kalucka, J., Bierhansl, L., Conchinha, N. V., Missiaen, R., Elia, I., Brüning, U., Scheinok, S., Treps, L., Cantelmo, A. R., Dubois, C. et al. (2018). Quiescent endothelial cells upregulate fatty acid β-oxidation for vasculoprotection via redox homeostasis. *Cell Metab.* **28**, 881-894.e13. doi:10.1016/j.cmet.2018.07.016
Kambadur, R., Koizumi, K., Stivers, C., Nagle, J., Poole, S. J. and Odenwald, W. F. (1998). Regulation of POU genes by castor and hunchback establishes layered compartments in the Drosophila CNS. *Gene Dev.* **12**, 246-260. doi:10.1101/gad.12.2.246
Kobayashi, T., Piao, W., Takamura, T., Kori, H., Miyachi, H., Kitano, S., Iwamoto, Y., Yamada, M., Imayoshi, I., Shioda, S. et al. (2019). Enhanced lysosomal degradation maintains the quiescent state of neural stem cells. *Nat. Commun.* **10**, 5446. doi:10.1038/s41467-019-13203-4
Kopan, R. and Ilagan, M. X. G. (2009). The canonical Notch signaling pathway: unfolding the activation mechanism. *Cell* **137**, 216-233. doi:10.1016/j.cell.2009.03.045
Lai, S.-L. and Doe, C. Q. (2014). Transient nuclear Prospero induces neural progenitor quiescence. *eLife* **3**, e03363. doi:10.7554/eLife.03363
Lee, H.-K. P., Wright, A. P. and Zinn, K. (2009). Live dissection of Drosophila embryos: streamlined methods for screening mutant collections by antibody staining. *J. Vis. Exp.* **34**, 1647. doi:10.3791/1647
Leevers, S. J., Weinkove, D., MacDougall, L. K., Hafen, E. and Waterfield, M. D. (1996). The Drosophila phosphoinositide 3-kinase Dp110 promotes cell growth. *EMBO J.* **15**, 6584-6594. doi:10.1002/j.1460-2075.1996.tb01049.x
Lehmann, R., Jiménez, F., Dietrich, U. and Campos-Ortega, J. A. (1983). On the phenotype and development of mutants of early neurogenesis inDrosophila melanogaster. *Wilhelm Roux's Arch. Dev. Biol.* **192**, 62-74. doi:10.1007/BF00848482
Leonardi, J., Fernandez-Valdivia, R., Li, Y.-D., Simcox, A. A. and Jafar-Nejad, H. (2011). Multiple O-glucosylation sites on Notch function as a buffer against temperature-dependent loss of signaling. *Development* **138**, 3569-3578. doi:10.1242/dev.068361
Li, S., Koe, C. T., Tay, S. T., Tan, A. L. K., Zhang, S., Zhang, Y., Tan, P., Sung, W.-K. and Wang, H. (2017). An intrinsic mechanism controls reactivation of neural stem cells by spindle matrix proteins. *Nat. Commun.* **8**, 122. doi:10.1038/s41467-017-00172-9
Lin, S., Marin, E. C., Yang, C.-P., Kao, C.-F., Apenteng, B. A., Huang, Y., O'Connor, M. B., Truman, J. W. and Lee, T. (2013). Extremes of lineage plasticity in the Drosophila brain. *Curr. Biol.* **23**, 1908-1913. doi:10.1016/j.cub.2013.07.074
Maurange, C., Cheng, L. and Gould, A. P. (2008). Temporal transcription factors and their targets schedule the end of neural proliferation in Drosophila. *Cell* **133**, 891-902. doi:10.1016/j.cell.2008.03.034
Mohammad, K., Dakik, P., Medkour, Y., Mitrofanova, D. and Titorenko, V. I. (2019). Quiescence entry, maintenance, and exit in adult stem cells. *Int. J. Mol. Sci.* **20**, 2158. doi:10.3390/ijms20092158
Mumm, J. S., Schroeter, E. H., Saxena, M. T., Griesemer, A., Tian, X., Pan, D. J., Ray, W. J. and Kopan, R. (2000). A ligand-induced extracellular cleavage regulates γ-secretase-like proteolytic activation of Notch1. *Mol. Cell* **5**, 197-206. doi:10.1016/S1097-2765(00)80416-5
Neumann, C. J. and Cohen, S. M. (1998). Boundary formation in Drosophila wing: Notch activity attenuated by the POU protein nubbin. *Science* **281**, 409-413. doi:10.1126/science.281.5375.409
Noseda, M., Chang, L., McLean, G., Grim, J. E., Clurman, B. E., Smith, L. L. and Karsan, A. (2004). Notch activation induces endothelial cell cycle arrest and participates in contact inhibition: role of p21Cip1 repression. *Mol. Cell. Biol.* **24**, 8813-8822. doi:10.1128/MCB.24.20.8813-8822.2004
Otsuki, L. and Brand, A. H. (2018). Cell cycle heterogeneity directs the timing of neural stem cell activation from quiescence. *Science* **360**, 99-102. doi:10.1126/science.aan8795
Otsuki, L. and Brand, A. H. (2019). Dorsal-ventral differences in neural stem cell quiescence are induced by p57KIP2/Dacapo. *Dev. Cell* **49**, 293-300.e3. doi:10.1016/j.devcel.2019.02.015
Pahl, M. C., Doyle, S. E. and Siegrist, S. E. (2019). E93 integrates neuroblast intrinsic state with developmental time to terminate MB neurogenesis via autophagy. *Curr. Biol.* **29**, 750-762.e3. doi:10.1016/j.cub.2019.01.039
Pan, D. and Rubin, G. M. (1997). Kuzbanian controls proteolytic processing of Notch and mediates lateral inhibition during Drosophila and vertebrate neurogenesis. *Cell* **90**, 271-280. doi:10.1016/S0092-8674(00)80335-9
Parody, T. R. and Muskavitch, M. A. (1993). The pleiotropic function of Delta during postembryonic development of Drosophila melanogaster. *Genetics* **135**, 527-539. doi:10.1093/genetics/135.2.527
Rebay, I., Fleming, R. J., Fehon, R. G., Cherbas, L., Cherbas, P. and Artavanis-Tsakonas, S. (1991). Specific EGF repeats of Notch mediate interactions with Delta and serrate: Implications for notch as a multifunctional receptor. *Cell* **67**, 687-699. doi:10.1016/0092-8674(91)90064-6
Shang, X., Wang, J., Luo, Z., Wang, Y., Morandi, M. M., Marymont, J. V., Hilton, M. J. and Dong, Y. (2016). Notch signaling indirectly promotes chondrocyte hypertrophy via regulation of BMP signaling and cell cycle arrest. *Sci. Rep.* **6**, 25594. doi:10.1038/srep25594
Siegrist, S. E., Haque, N. S., Chen, C.-H., Hay, B. A. and Hariharan, I. K. (2010). Inactivation of both Foxo and reaper promotes long-term adult neurogenesis in Drosophila. *Curr. Biol.* **20**, 643-648. doi:10.1016/j.cub.2010.01.060
Sipe, C. W. and Siegrist, S. E. (2017). Eyeless uncouples mushroom body neuroblast proliferation from dietary amino acids in Drosophila. *eLife* **6**, e26343. doi:10.7554/eLife.26343
Sousa-Nunes, R., Yee, L. L. and Gould, A. P. (2011). Fat cells reactivate quiescent neuroblasts via TOR and glial insulin relays in Drosophila. *Nature* **471**, 508-512. doi:10.1038/nature09867
Spéder, P. and Brand, A. H. (2018). Systemic and local cues drive neural stem cell niche remodelling during neurogenesis in Drosophila. *eLife* **7**, e30413. doi:10.7554/eLife.30413
Sriuranpong, V., Borges, M. W., Ravi, R. K., Arnold, D. R., Nelkin, B. D., Baylin, S. B. and Ball, D. W. (2001). Notch signaling induces cell cycle arrest in small cell lung cancer cells. *Cancer Res.* **61**, 3200-3205.
Sueda, R. and Kageyama, R. (2020). Regulation of active and quiescent somatic stem cells by Notch signaling. *Dev. Growth Differ.* **62**, 59-66. doi:10.1111/dgd.12626
Truman, J. W. and Bate, M. (1988). Spatial and temporal patterns of neurogenesis in the central nervous system of Drosophila melanogaster. *Dev. Biol.* **125**, 145-157. doi:10.1016/0012-1606(88)90067-X
Tsuji, T., Hasegawa, E. and Isshiki, T. (2008). Neuroblast entry into quiescence is regulated intrinsically by the combined action of spatial Hox proteins and temporal identity factors. *Development* **135**, 3859-3869. doi:10.1242/dev.025189
Ulvklo, C., MacDonald, R., Bivik, C., Baumgardt, M., Karlsson, D. and Thor, S. (2012). Control of neuronal cell fate and number by integration of distinct daughter cell proliferation modes with temporal progression. *Development* **139**, 678-689. doi:10.1242/dev.074500
Urbán, N., Blomfield, I. M. and Guillemot, F. (2019). Quiescence of adult mammalian neural stem cells: a highly regulated rest. *Neuron* **104**, 834-848. doi:10.1016/j.neuron.2019.09.026
Vaccari, T., Lu, H., Kanwar, R., Fortini, M. E. and Bilder, D. (2008). Endosomal entry regulates Notch receptor activation in Drosophila melanogaster. *J. Cell Biol.* **180**, 755-762. doi:10.1083/jcb.200708127
Yang, C.-P., Samuels, T. J., Huang, Y., Yang, L., Ish-Horowicz, D., Davis, I. and Lee, T. (2017). Imp and Syp RNA-binding proteins govern decommissioning of Drosophila neural stem cells. *Development* **144**, 3454-3464. doi:10.1242/dev.149500
Yuan, X., Sipe, C. W., Suzawa, M., Bland, M. L. and Siegrist, S. E. (2020). Dilp-2–mediated PI3-kinase activation coordinates reactivation of quiescent neuroblasts with growth of their glial stem cell niche. *PLoS Biol.* **18**, e3000721. doi:10.1371/journal.pbio.3000721
Zacharioudaki, E., Magadi, S. S. and Delidakis, C. (2012). bHLH-O proteins are crucial for Drosophila neuroblast self-renewal and mediate Notch-induced overproliferation. *Development* **139**, 1258-1269. doi:10.1242/dev.071779
Zhang, R., Boareto, M., Engler, A., Louvi, A., Giachino, C., Iber, D. and Taylor, V. (2019). Id4 Downstream of Notch2 maintains neural stem cell quiescence in the adult hippocampus. *Cell Rep.* **28**, 1485-1498.e6. doi:10.1016/j.celrep.2019.07.014
Zielke, N., Korzelius, J., van Straaten, M., Bender, K., Schuhknecht, G. F. P., Dutta, D., Xiang, J. and Edgar, B. A. (2014). Fly-FUCCI: a versatile tool for studying cell proliferation in complex tissues. *Cell Rep.* **7**, 588-598. doi:10.1016/j.celrep.2014.03.020

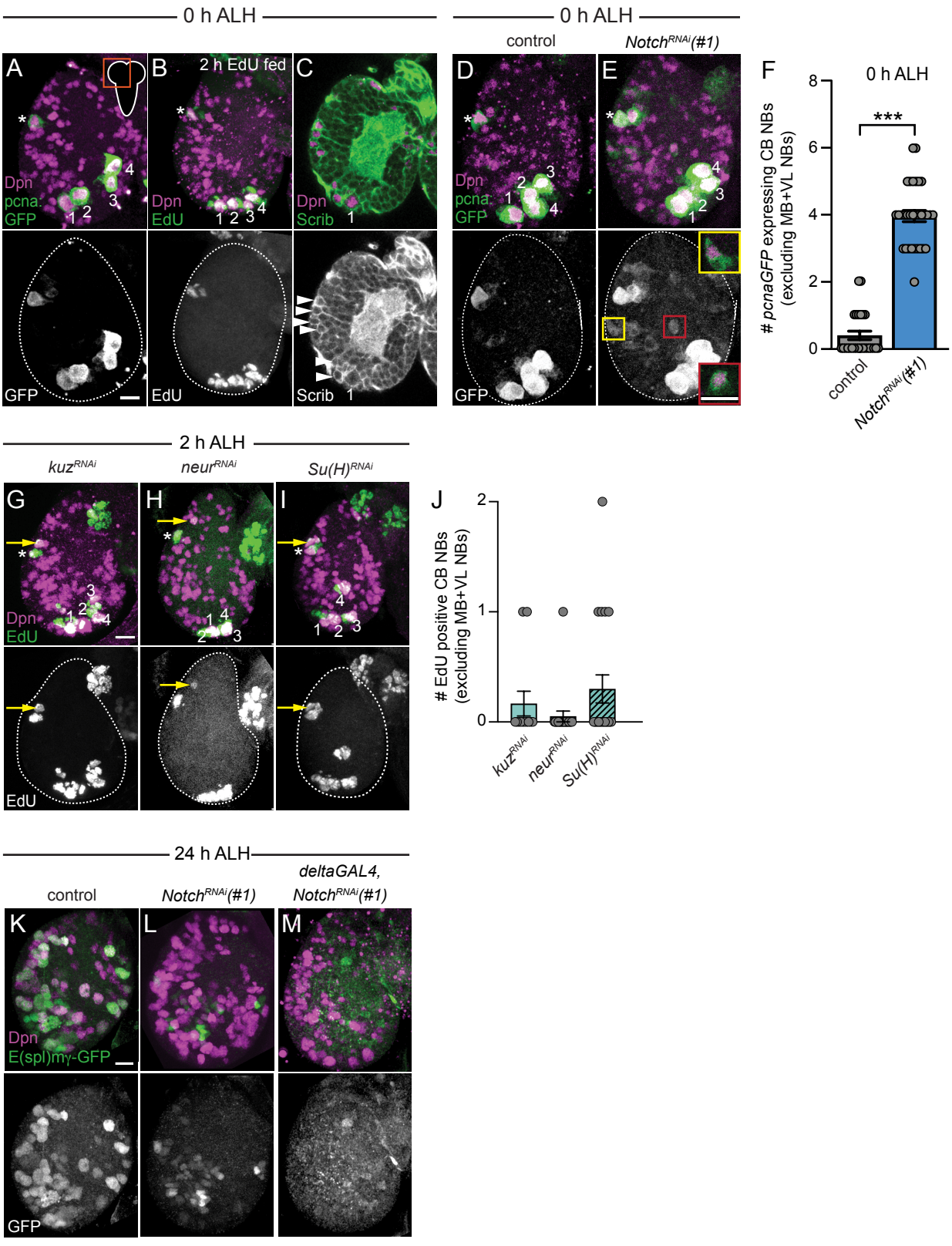

Fig. S1. CB NBs are quiescent and small in the newly hatched larvae.

(A-B, D-E, G-I, K-M) Maximum intensity projections of single brain hemispheres from indicated genotypes and timepoints showing *pcna:GFP* expression (A, D-E), EdU incorporation after 2 hours of larval EdU treatment (B, G-I), *E(spl)mγ-GFP* reporter expression (K-M). Top panels are colored overlays with single channel grayscale images below. Numbers 1-4 indicate the MB NBs and the white asterisk indicates the VL NB (A-B, D-E, G-I). Boxes (E) indicate ectopic *pcnaGFP* expressing CB NBs. (C) Single optical section to show cell size difference in proliferating MB NB (indicated by number 1) and quiescent CB NBs (indicated by white arrowheads). Top panels are colored overlays with single channel grayscale images below. (F) Quantification of *pcnaGFP* expressing CB NBs (excluding MB+VL NBs) for the indicated genotypes at 0 hrs ALH. Each data point represents one brain hemisphere. Mean and SEM. ***p≤0.001 (Student two-tailed t-test). (J) Quantification of EdU positive CB NBs (excluding MB+VL NBs) in the indicated genotypes after two hours of larval EdU treatment. Each data point represents one brain hemisphere. Mean and SEM. Scale bar equals 10 μms. See Supp. Table 2 for panel genotypes.

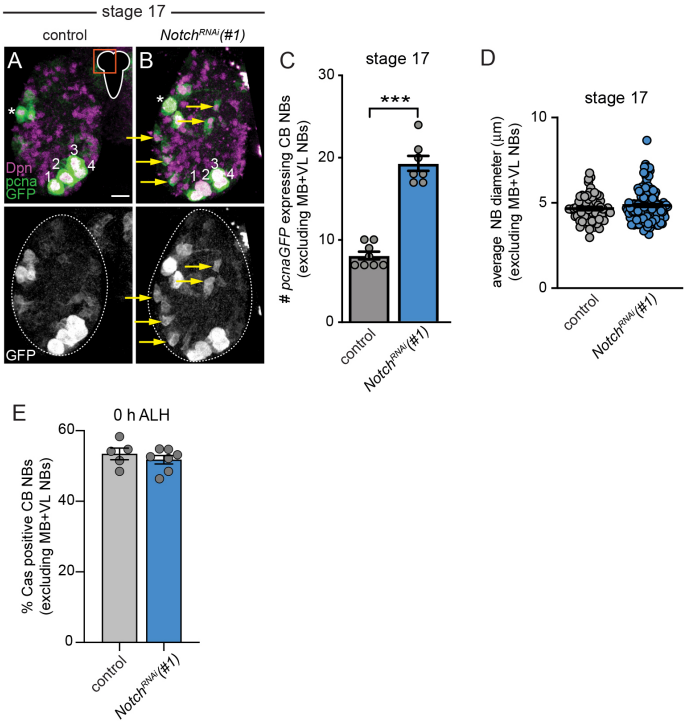

Fig. S2. Notch signaling regulates the timing of CB NBs entry into quiescence.

(A-B) Maximum intensity projections of single brain hemispheres from indicated genotypes at embryonic stage 17 showing *pcna:GFP* expression. Top panels are colored overlays with single channel grayscale image below. Numbers 1-4 indicate the MB NBs; the white asterisk indicates the VL NB and the yellow arrows indicate ectopic *pcna:GFP* expression in CB NBs. (C) Quantification of *pcnaGFP*-expressing CB NBs (excluding MB+VL NBs) for the indicated genotypes at embryonic stage 17. Each data point represents one brain hemisphere. Mean and SEM. ***p≤0.001 (Student two-tailed t-test). (D) Quantification of CB NBs (excluding MB+VL NBs) size for indicated genotypes at embryonic stage 17. Each data point represents individual NB from n=4 animals. Mean and SEM. (E) Quantification of Cas-expressing CB NBs (excluding MB+VL NBs) for indicated genotypes at 0 hr ALH. Each data point represents one brain hemisphere. Mean±SEM. Scale bar equals 10 µms. See Supp. Table 2 for panel genotypes.

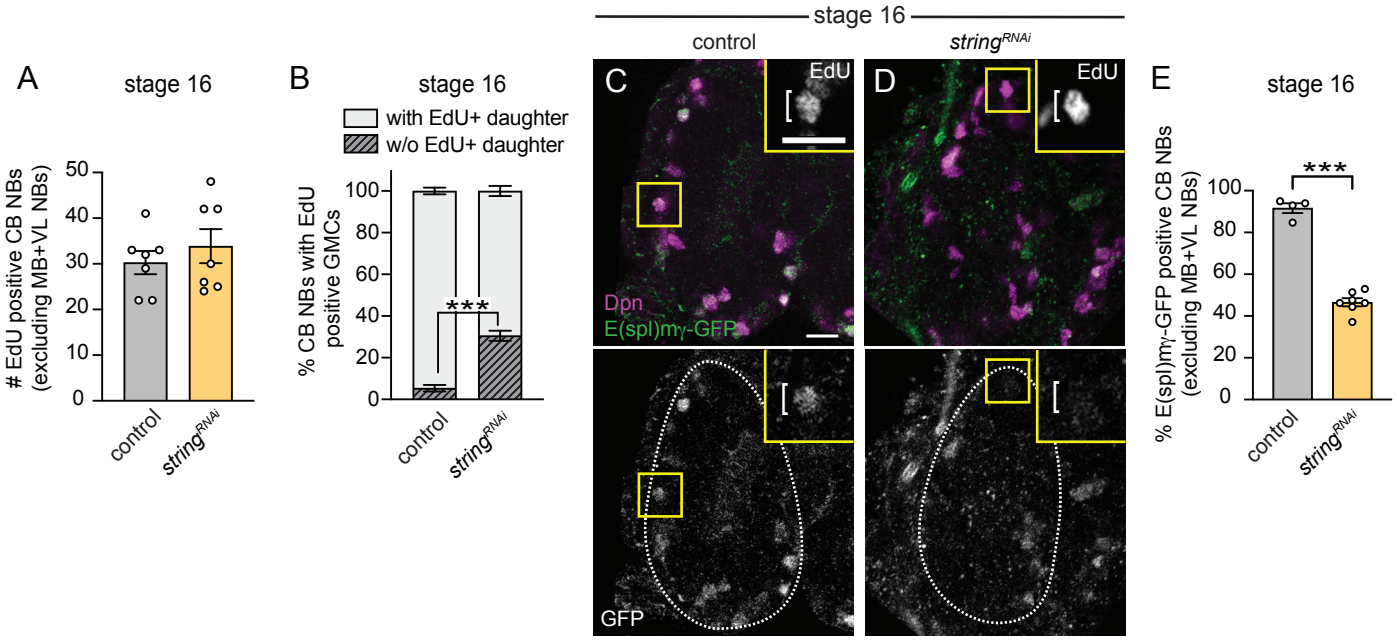

Fig. S3. Notch signaling is active in proliferating, but not cell cycle arrested CB NBs. (A) Quantification of the number of EdU incorporating CB NBs (excluding MB+VL NBs) from indicated genotypes after 1 hour of EdU treatment at embryonic stage 16. Each data point represents one brain hemisphere. Mean and SEM. (B) Quantification of the percent of EdU positive CB NBs (excluding MB+VL NBs) with or without the presence of an EdU positive daughter cell from indicated genotypes at embryonic stage 16. Data represents mean and SEM from n=5 animals. ***p≤0.001 (Two-way ANOVA). (C-D) Single optical section of a brain hemisphere from indicated genotypes showing expression of *E(spl)mγ-GFP* at embryonic stage 16. Top panels are colored overlays with single channel grayscale images below. Insets show higher magnification images of the CB NBs highlighted by the yellow box. (E) Quantification of the percent of CB NBs (excluding MB+VL NBs) expressing *E(spl)mγ-GFP* from indicated genotypes at embryonic stage 16. Each data point represents one brain hemisphere. Mean and SEM. ***p≤0.001 (Student two-tailed t-test). Scale bar equals 10 μms. See Supp. Table 2 for panel genotypes.

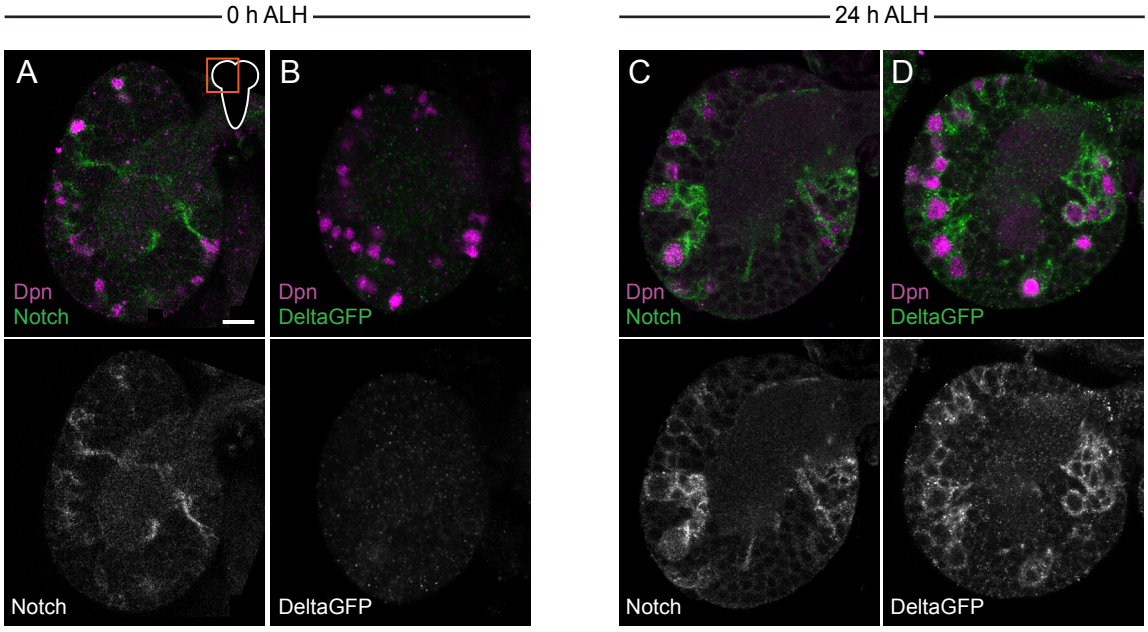

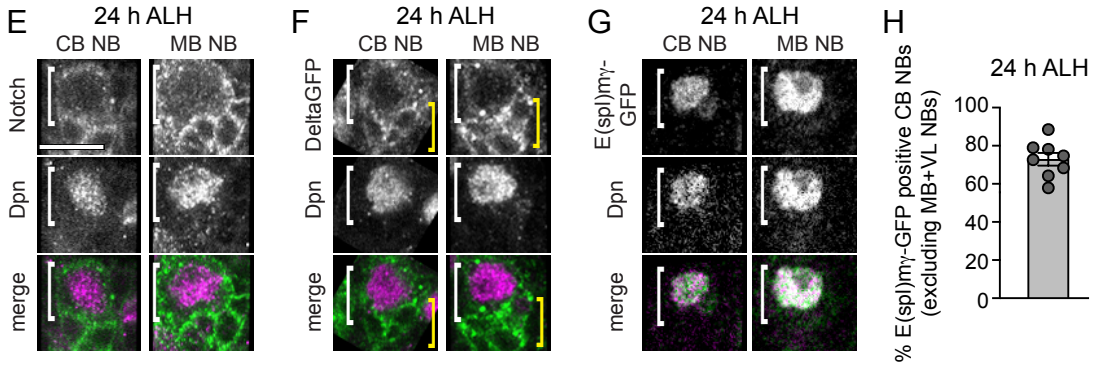

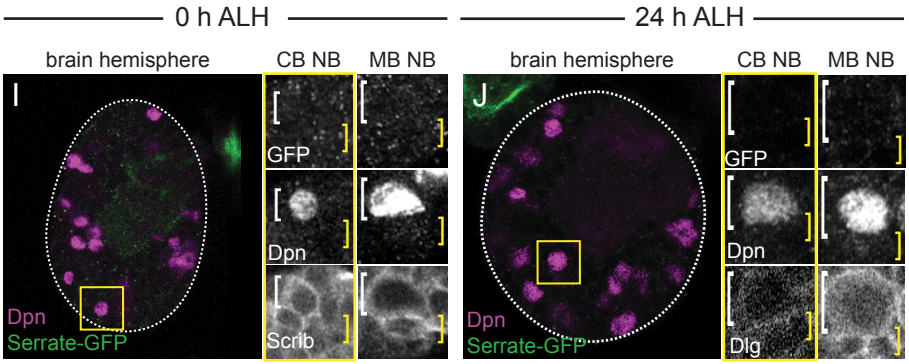

Fig. S4. Notch signaling is active in reactivated CB NBs.

(A-D) Single optical section of a brain hemisphere from wild type animals at indicated timepoints showing expression of Notch ICD antibody (A, C) and *DeltaGFP* (B, D). Top panels are colored overlays with single channel grayscale images below. (E-G) Single optical section of wildtype CB NBs and MB NBs showing expression of Notch ICD antibody (E), *DeltaGFP* (F) and *E(spl)mγ-GFP* (G) at 24 hours ALH. White brackets indicate the neuroblast and the yellow brackets indicate the new born GMCs. Top panels are single channel grayscale images with the colored overlay below. (H) Quantification of the percent of CB NBs (excluding MB+VL NBs) expressing *E(spl)mγ-GFP* at 24 hours ALH. Each data point represents one brain hemisphere. Mean and SEM. (I-J) Single optical sections of a brain hemisphere from animals expressing *Serrate:GFP*. Brain hemispheres are outlined. Panels on the right show single channel grayscale images of the CB NB (marked by a yellow box) and MB NB from the same brain hemisphere at a higher magnification. Scale bar equals 10 μms. See Supp. Table 2 for panel genotypes.

Table S1. Fly stocks

Genotype:	Source:	Identifier:
Oregon R	Bloomington Drosophila Stock Center	5
wor-Gal4	(Albertson and Doe, 2003)	
tubulin-Gal80(ts)	Bloomington Drosophila Stock Center	7108
GMR25B11-Gal4 (delta-Gal4)	Bloomington Drosophila Stock Center	46170
Kuzbanian^{e29-4}	Bloomington Drosophila Stock Center	5804
Cas^{24}	(Cui and Doe, 1992)	
UAS-Notch RNAi (HMS00001)	Bloomington Drosophila Stock Center	33611
UAS-Notch RNAi (HMS00009)	Bloomington Drosophila Stock Center	33616
UAS-Su(H)RNAi (HMS05748)	Bloomington Drosophila Stock Center	67928
UAS-neuralized RNAi (HMS05744)	Bloomington Drosophila Stock Center	67917
UAS-Kuzbanian RNAi (HMS05424)	Bloomington Drosophila Stock Center	66958
UAS-tribbles RNAi (HMS04999)	Bloomington Drosophila Stock Center	60007
UAS-hippo RNAi (HMS00006)	Bloomington Drosophila Stock Center	33614
UAS-dacapo RNAi (HMS05632)	Bloomington Drosophila Stock Center	64026
UAS-dp110	(Leevers et al., 1996)	
UAS-numb RNAi (HMS01459)	Bloomington Drosophila Stock Center	35045
UAS-Notch$^{\Delta EXT}$	Bloomington Drosophila Stock Center	63220
UAS-string RNAi (HMS00146)	Bloomington Drosophila Stock Center	34831
UAS-Fucci	Bloomington Drosophila Stock Center	55101
UAS-Notch^{ICD}	(Go et al., 1998)	
E(spl)mγ-GFP	(Almeida and Bray, 2005)	
Delta-GFP	Bloomington Drosophila Stock Center	59819
Serrate-GFP	Bloomington Drosophila Stock Center	59824
pcna-GFP	(Thacker et al., 2003)	

Table S2. Genotypes listed by figure panel

Figure	Genotype	
Figure 1B	*worGal4/+ (Oregon R)*	control
Figure 1C	*worGal4/+; UAS-Notch RNAi (HMS00001)/+*	
Figure 1D	*worGal4/+; UAS-Notch RNAi (HMS00009)/+*	
Figure 1E	*Kuzbanian^{e29-4}/Kuzbanian^{e29-4}*	
Figure 1F	*deltaGal4/UAS-Notch RNAi (HMS00001)*	
Figure 2A, F	*worGal4/+ (Oregon R)*	control
Figure 2B, G	*worGal4/+; UAS-Notch RNAi (HMS00001)/+*	
Figure 2C	*worGal4/+; UAS-N$^{\Delta EXT}$ /+*	
Figure 3B	*worGal4/+; UAS-Fucci/+ (Oregon R)*	control
Figure 3C	*worGal4/+; UAS-Fucci/ UAS-Notch RNAi (HMS00001)*	
Figure 3E	*worGal4, UAS-dp110/+; UAS-Notch RNAi (HMS00001)/+*	
Figure 3F	*worGal4, tubGal80$^{(ts)}$/ +; UAS-Notch RNAi (HMS00001)/+*	control
Figure 3G	*worGal4, tubGal80$^{(ts)}$/+; UAS-Notch RNAi (HMS00001)/ UAS-hpo RNAi*	
Figure 3H	*worGal4, tubGal80$^{(ts)}$/ UAS-trbls RNAi; UAS-Notch RNAi (HMS00001)/+*	
Figure 3I	*worGal4, tubGal80$^{(ts)}$/ UAS-dap RNAi; UAS-Notch RNAi (HMS00001)/+*	
Figure 4A, B, D	*E(spl)mγ-GFP/ E(spl)mγ-GFP*	control
Figure 4F, G	*E(spl)mγ-GFP; Cas^{24}/E(spl)mγ-GFP; Cas^{24}*	
Figure 4J	*worGal4/+; pcna:GFP/+ (Oregon R)*	control
Figure 5A	*Oregon R*	control
Figure 5B, C, F	*Delta-GFP/+*	control
Figure 5E	*E(spl)mγ-GFP/ E(spl)mγ-GFP*	control
Figure 6A, D, F	*worGal4/+; E(spl)mγ-GFP/UAS-numb RNAi*	
Figure 6C	*Oregon R*	control
Figure 7B	*wornGal4; Cas^{24}/UAS-Notch^{ICD}; Cas^{24}*	
Suppl. Fig. 1A, D	*worGal4/+; pcna:GFP/+ (Oregon R)*	control
Suppl. Fig. 1B, C	*worGal4/+ (Oregon R)*	control

Suppl. Fig. 1E	*worGal4/+; pcna:GFP/ UAS-Notch RNAi (HMS00001)*	
Suppl. Fig. 1G	*worGal4/UAS-Kuzbanian RNAi (HMS05424)*	
Suppl. Fig. 1H	*worGal4/UAS-neuralized RNAi (HMS05744)*	
Suppl. Fig. 1I	*worGal4/UAS-Su(H)RNAi (HMS05748)*	
Suppl. Fig. 1K	*worGal4/+; E(spl)mγ-GFP /+ (Oregon R)*	control
Suppl. Fig. 1L	*worGal4/+; E(spl)mγ-GFP / UAS-Notch RNAi (HMS00001)*	
Suppl. Fig. 1M	*E(spl)mγ-GFP/+; deltaGal4/ UAS-Notch RNAi (HMS00001)*	
Suppl. Fig. 2A	*worGal4/+; pcna:GFP/+ (Oregon R)*	control
Suppl. Fig. 2B	*worGal4/+; pcna:GFP/ UAS-Notch RNAi (HMS00001)*	
Suppl. Fig. 3C	*worGal4/+; E(spl)mγ-GFP /+ (Oregon R)*	control
Suppl. Fig. 3D	*worGal4/+; E(spl)mγ-GFP /UAS-string RNAi*	
Suppl. Fig. 4A, C, E	Oregon R	control
Suppl. Fig. 4B, D, F	*Delta-GFP/+*	control
Suppl. Fig. 4G	*E(spl)mγ-GFP/ E(spl)mγ-GFP*	control
Suppl. Fig. 4I, J	*Serrate-GFP/+*	

Albertson, R. and Doe, C. Q. (2003). Dlg, Scrib and Lgl regulate neuroblast cell size and mitotic spindle asymmetry. *Nat Cell Biol* 5, 166–170.

Almeida, M. S. and Bray, S. J. (2005). Regulation of post-embryonic neuroblasts by Drosophila Grainyhead. *Mech Develop* 122, 1282–1293.

Cui, X. and Doe, C. Q. (1992). ming is expressed in neuroblast sublineages and regulates gene expression in the Drosophila central nervous system. *Development* 116, 943–952.

Go, M. J., Eastman, D. S. and Artavanis-Tsakonas, S. (1998). Cell proliferation control by Notch signaling in Drosophila development. *Dev Camb Engl* 125, 2031–40.

Leevers, S. J., Weinkove, D., MacDougall, L. K., Hafen, E. and Waterfield, M. D. (1996). The Drosophila phosphoinositide 3-kinase Dp110 promotes cell growth. *Embo J* 15, 6584–6594.

Thacker, S. A., Bonnette, P. C. and Duronio, R. J. (2003). The Contribution of E2F-Regulated Transcription to Drosophila PCNA Gene Function. *Curr Biol* 13, 53–58.